J Solution Chem (2017) 46:720–733
DOI 10.1007/s10953-017-0595-x

# Solvent Effects on Acid–Base Equilibria of Propranolol and Atenolol in Aqueous Solutions of Methanol: UV-Spectrophotometric Titration and Theory

**Mehran Abbaszadeh Amirdehi[1] · Mohammad Pousti[1] · Farnaz Asayesh[1] · Farrokh Gharib[2] · Jesse Greener[1]**

Received: 18 August 2016 / Accepted: 16 January 2017 / Published online: 20 March 2017


**Abstract** The p$K_a$ values of two important drugs were determined in different binary aqueous/organic solutions, which mimic a range of industrial solvents and biological fluids encountered during drug synthesis and end use. Titrations of monoprotic (propranolol) and diprotic (atenolol) drugs were determined using a combination of potentiometric and spectroscopic methods at constant temperature and ionic strength. Single-parameter correlations between the measured p$K_a$ values (at 25 °C) and hydrogen-bond acidity/basicity or solvent polarity parameters were poor in all cases. However, analysis using the multi-parameter method of Kamlet, Abboud, and Taft represents significant improvement enabling better interpretation of the solvent effects on the acid−base equilibria of the drugs. As a validation step and for a deeper understanding of the origins of the solvent effects on the drugs, all p$K_a$ values were predicted by DFT calculations. Finally, acidity constants were determined by correlations between experimental and theoretical measurements. The developed method will measure and accurately simulate the effect of the solvent environment on p$K_a$ values and represent advancement for questions related to drug synthesis and drug compound's behavior in biological fluids.

**Electronic supplementary material** The online version of this article (doi:10.1007/s10953-017-0595-x) contains supplementary material, which is available to authorized users.

✉ Jesse Greener
Jesse.Greener@chm.ulaval.ca

[1] Département de Chimie, Université Laval, 1045 Avenue de La Médecine, Québec, QC G1V0A6, Canada

[2] Chemistry Department, Shahid Beheshti University, G. C., Evin, Tehran, Iran

***Graphical Abstract***

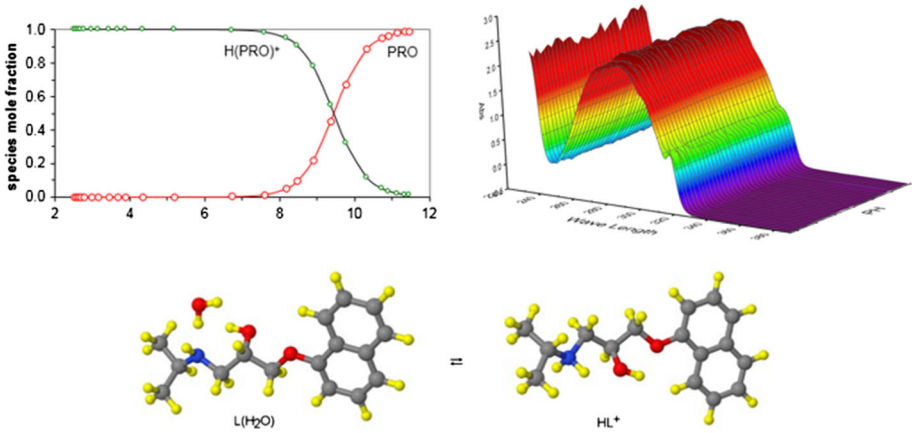


**Keywords** Protonation constant · Propranolol · Atenolol · Solvent effect · Kamlet and Taft Solvatochromic parameters · DFT

## 1 Introduction

Detailed knowledge of protonation constants of drug compounds is critical for understanding and predicting mechanisms of action. For example, fat-soluble (lipophilic) drugs diffuse through the cell membrane according to their charges [1, 2]. Added to this, the interaction between solvents with different polarities and certain molecules has been identified as an important factor in drug molecule interactions with DNA or active sites of enzymes, side chains in proteins or generally any binding action [3, 4]. In addition, knowledge of the p$K_a$ values in industrial solvents can benefit applications such as the design of liquid pharmaceutical dosages, as well as considerations in drug synthesis and testing such as solubility, purification and drug screening [5–7]. Therefore, solvent effects on drug molecule properties, particularly their p$K_a$ values, are very important. The dielectric constant ($\varepsilon$) of a solvent, which is related to the solvent polarity ($E_T$) through the Debye equation, is an important physicochemical property mostly analyzed in terms of its effect on drug p$K_a$. This has led to recent analytical initiatives to measure $E_T$ within biological microenvironments, in order to better predict the behavior of natural biomolecules and drug molecules [8–11]. However, the relationship between $E_T$ and p$K_a$ is not always straightforward, and cannot be used reliably to extrapolate drug molecule behavior in new biochemical environments. Therefore, the multi-parameter model proposed by Kamlet, Abboud, and Taft (KAT) has gained interest among researchers, due to its ability to account for the basic modes of solute–solvent interactions. These include hydrogen-bond acidity ($\alpha$), hydrogen-bond basicity ($\beta$) and dipolarity/polarizability ($\pi^*$). To facilitate this approach, a general method to modulate easily the solution properties to mimic a range of solvent environments was achieved using aqueous–organic solvent combinations as multipurpose solvents to emulate a wide range of physiochemical properties [12].

Recently, such binary solvents were used to study physiochemical properties such as solubility and acid–base properties of a range of solutes including fluorescent probes, naturally occurring biomolecules and their complexes with foreign species [13–17].

The aim of the present study is to use different binary aqueous/organic solvents as a means to comprehensively study the effect of solvents on the KAT parameters to describe the variation of $pK_a$ of mono- and diprotic drug compounds. In addition, computer simulations are used to validate the experimental results and give deeper insight into reaction mechanisms for protonation/deprotonation phenomena and the most probable equilibrium reaction mechanisms between protonated and deprotonated states. We chose the monoprotic and diprotic drug compounds propranolol (PRO) and atenolol (ATN) (Fig. 1), respectively, because they are well-known β-adreno receptor blocking agents, also used to treat hypertension, angina, arrhythmias, anxiety management, migraine prophylaxis, hyperthyroidism and tremors [18]. Propranolol, for example, is considered an essential drug for treating migraine headaches by the World Health Organization [19].

## 2 Experimental

### 2.1 Chemicals

PRO and ATN, were obtained from Fluka as analytical reagent grade materials (98 and 95%, respectively) and they were used without further purification. Methanol (99.8%) and perchloric acid (99%) were purchased from Merck (reagent grade materials) and were used as received. Sodium perchlorate ($NaClO_4$) was supplied from Merck and was dried at room temperature for at least 48 h under vacuum before use. NaOH solution was prepared from a titrisol solution (Merck). All dilute solutions were prepared with $CO_2$-free and de-ionized water with a conductance equal to $1.3 \pm 0.1$ $\mu S \cdot cm^{-1}$.

### 2.2 Apparatus

Electromotive force (emf) measurements of all solutions were made using a pH ion-meter, Metrohm model 781, equipped with a glass-pH electrode (model 6.0258.000) that was modified by replacing its aqueous KCl solution with a solution consisting of 0.01 M NaCl + 0.09 M $NaClO_4$, saturated with AgCl. The electrode was soaked for (15–20) min in the water–organic solvent mixture before the potentiometric measurements. All titrations were carried out in an 80 mL capacity thermostated double-walled glass vessel at 25°C. In this work, the ionic strengths of all solutions were adjusted to 0.1 $mol \cdot dm^{-3}$ with $NaClO_4$. A peristaltic pump was used to circulate the solutions from the titration vessel to the spectrophotometric cell through Teflon or Tygon tubes, so the whole process was automated with continuous flow and the solution absorbance could be measured simultaneously with the emf. Spectrophotometric measurements were recorded with a UV–Vis

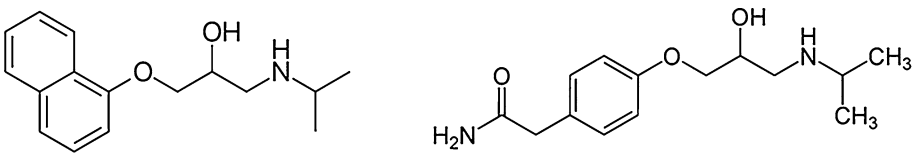


**Fig. 1** Chemical structures of propranolol (*left*) and atenolol (*right*)

Shimadzu 2100 spectrophotometer, controlled with a computer. UV–Vis sampling was accomplished through thermostated 10 mm flow-through quartz cells. To avoid formation of carbonate and carbonic acid by dissolved $CO_2$, which could have affected the pH, we bubbled ultrapure $N_2$ through the reaction solution. Absorbance measurements were made in the spectral window of 200–400 nm with spectral resolution of 0.5 nm. The measured emf was related to solution pH as described in the supplementary information. The spectrophotometric titrations were analyzed with the Squad computer program which is based on titration curves [20, 21].

## 2.3 Computational Details

All calculations of neutral and cationic forms of the drug molecules and water cluster molecules were carried out using the GAMESS-US version May 1, 2013 (R1) [22]. Geometry optimizations and frequency calculations were performed at the B3LYP/6-311++G(d,p) level of theory. To include the solvent effect in our calculation, solvation model density (SMD) was used. The SMD solvation model was used to calculate solute–solvent interactions in different binary mixtures of water and methanol. The SMD model calculates short-range interaction energies between solvent and solute in different binary mixtures of water and methanol by using a modified solvent-accessible surface area that incorporates parameters for atomic and molecular surface tensions and hydrogen-bond acidity and basicity [23, 24].

For building the structure and visualizing all species involved in the reactions, Gabedit v2.4.0 [25], Jmolv13.0.16 [26] and wxMacMolPltv7.4.4 [27] programs were used. At first, all proposed geometries were fully optimized without any geometrical constraint and then vibrational tests were conducted to make sure that there are no imaginary frequencies for the optimized structures. A cluster continuum method which takes advantage of both implicit and explicit solvent molecules were used to simulate different binary mixtures of methanol–water for calculating $pK_a$ values [28]. In this explicit approach only water molecules are accounted for. On the other hand, in this implicit approach water is considered as a main solvent in SMD model with the effect of methanol in the binary mixtures added to water solvent considered by changing the dielectric constant of water to the experimental values reported in Table 1. For calculating $pK_a$ values, several reactions were tested; some of the reactions were not considered further due to large deviations from the experimental results.

### *2.3.1 Fitting*

$pK_a$ values were correlated with the KAT solvent properties by means of multiple regression analysis using the Gauss–Newton non-linear least-squares method by a suitable computer program (Microsoft Excel Solver and Linest) [29]. Further information is given in the supporting information file. We refined the $pK_a$ values by minimizing the error squares sum from Eq. 1:

$$U = \sum \left(pK_{exp} - pK_{fitting}\right)^2. \quad (1)$$

**Table 1** The comparison of B3LYP-SMD/6-311++G (d,p) calculated and experimental $pK_a$ values of PRO and ATN (at 25 °C)

| | | Experimental | | | Theoretical | | |
|---|---|---|---|---|---|---|---|
| Methanol % (v/v) | Dielectric constants ($\varepsilon$) | $pK_{aPRO}$ | $pK_{aATN1}$ | $pK_{aATN2}$ | $pK_{aPRO}$ | $pK_{aATN1}$ | $pK_{aATN2}$ |
| 0 | 79.5 | 9.43 ± 0.02 | 9.49 ± 0.02 | 3.59 ± 0.04 | 9.78 ± 0.037 | 9.50 ± 0.001 | 3.76 ± 0.047 |
| 10 | 76.4 | 9.38 ± 0.02 | 9.41 ± 0.02 | 3.55 ± 0.03 | 9.57 ± 0.020 | 9.36 ± 0.005 | 3.51 ± 0.011 |
| 15 | 74.5 | 9.33 ± 0.01 | 9.37 ± 0.02 | 3.53 ± 0.05 | 9.51 ± 0.019 | 9.30 ± 0.008 | 3.46 ± 0.020 |
| 20 | 72.1 | 9.27 ± 0.03 | 9.33 ± 0.03 | 3.50 ± 0.01 | 9.47 ± 0.022 | 9.25 ± 0.009 | 3.39 ± 0.031 |
| 25 | 71.0 | 9.24 ± 0.01 | 9.29 ± 0.01 | 3.48 ± 0.02 | 9.42 ± 0.019 | 9.19 ± 0.011 | 3.34 ± 0.040 |
| 30 | 68.3 | 9.19 ± 0.01 | 9.21 ± 0.01 | 3.44 ± 0.01 | 9.38 ± 0.021 | 9.15 ± 0.007 | 3.29 ± 0.044 |
| 35 | 67.2 | 9.18 ± 0.02 | 9.20 ± 0.04 | 3.42 ± 0.02 | 9.32 ± 0.015 | 9.10 ± 0.011 | 3.24 ± 0.053 |
| 40 | 65.8 | 9.15 ± 0.03 | 9.12 ± 0.02 | 3.39 ± 0.03 | 9.27 ± 0.013 | 9.04 ± 0.009 | 3.2 ± 0.056 |
| 45 | 63.0 | 9.10 ± 0.04 | 9.08 ± 0.01 | 3.32 ± 0.01 | 9.21 ± 0.012 | 8.98 ± 0.011 | 3.15 ± 0.051 |
| 50 | 60.8 | 9.04 ± 0.03 | 9.04 ± 0.04 | 3.28 ± 0.05 | 9.15 ± 0.012 | 8.93 ± 0.012 | 3.09 ± 0.058 |
| %MRD | | | | | 0.19 | 0.09 | 0.41 |
| 0 | | 9.49 | 9.40 | | Ref. [30] | | |
| 0 | | 9.45 | 9.6 | | Ref. [31][a] | | |
| 0 | | | 9.48 | | Ref. [32][b] | | |

The relative deviation values of theoretical and experimental results for each $pK_a$ are reported. Also the percentages of MRD for each $pK_a$ are given

[a] Potentiometric titration method at temperature ($t$ = 21–24 °C)

[b] Potentiometric titration at constant ionic strength ($I$ = 0.15 mol·dm$^{-3}$ KCl) and temperature ($t$ = 25.0 ± 0.5 °C)

## 3 Results and Discussion

### 3.1 Titrations

The speciation of drugs in the aqueous solution can be readily illustrated by their distribution curves as a function of $p_cH$. In this work, the fractions of various forms of representative drugs, such as $H_2ATN^{2+}$, $HATN^{+}$, ATN (Fig. 2a) and $HPRO^{+}$, PRO (Fig. 2b) are depicted in Fig. 2. For ATN, the results indicate that in the pH range of 3–4, the major species are $H_2ATN^{2+}$, $HATN^{+}$, in the 8–10 pH range the major species are $HATN^{+}$, ATN and PRO (Fig. 2a, b), while at pHs > 10 the dominant species are neutral ATN and PRO. The speciation of these drugs in binary solutions significantly impacts biomicro environment-related processes such as metal complexation, decomposition, drug–solvents, proteins and cell interactions. The $pK_a$ values were measured from titration curves, by drop wise addition of NaOH to the drug solution in the concentration range 1.0–3.0 mmol·dm$^{-3}$. Both titrate and titrant had the same percentages of methanol for each titration run.

For minimizing the sums of the squares of the deviations of the experimental absorbances from the calculated ones, the measured absorbance and pcH data from the titration in the computer program were fitted with Eqs. 2–4:

$$H_2(ATN)^{2+} \rightleftharpoons H(ATN)^{+} + H^{+} K_1 = [H(ATN)^{+}][H^{+}]/[H_2(ATN)^{2+}] \quad (2)$$

$$H(ATN)^{+} \rightleftharpoons ATN + H^{+} K_2 = [ATN]\,[H^{+}]/[H(ATN)^{+}] \quad (3)$$

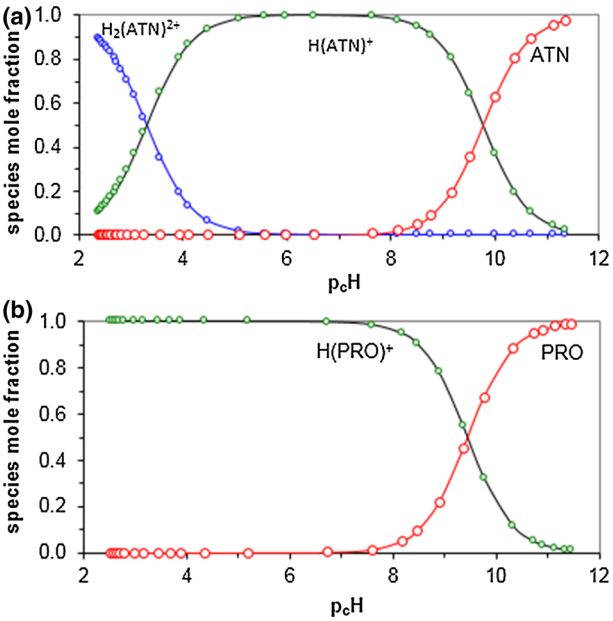


**Fig. 2** Equilibrium distribution of different protonation states of ATN (**a**) and PRO (**b**) as a function of pcH in water (0% methanol). *Blue*, *green*, and *red circles* represent doubly, singly and non-protonated molecules, respectively (Color figure online)

$$H(PRO)^{+} \rightleftharpoons PRO + H^{+} K = [PRO]\,[H^{+}]/[H(PRO)^{+}] \quad (4)$$

Since PRO is monoprotic and ATN is diprotic, one $pK_a$ value was extracted from the titration of PRO ($pK_{aPRO}$), whereas two $pK_a$ values were obtained from the titration of ATN ($pK_{aATN1}$, $pK_{aATN2}$) by fitting the calculated UV–Vis adsorption values to experimental ones (the chosen wavelengths were around 250 nm). $pK_{aPRO}$, $pK_{aATN1}$, $pK_{aATN2}$ are listed in Table 1 together with some values reported in the literature [30–32]. Titrations were performed for ATN and PRO solutions in binary solvents with different water–methanol mixing ratios to explore the solvent effect on the $pK_a$ values. The UV–Vis spectra of propranolol and atenolol in 30% water–methanol are shown in Fig. 3.

### 3.2 Solvent Effect

In general, the standard Gibbs energy of acid–base equilibria consists of an electrostatic term, which can be estimated by the Born equation (S5), and a non-electrostatic term, which includes specific solute–solvent interaction [33, 34]. When the electrostatic effects predominate (as in case of $pK_{aATN2}$), then the plot of $pK_a$ versus $\varepsilon^{-1}$ of the media should be linear. As seen in Fig. 4, the correlation between $pK_{aATN2}$ and $\varepsilon^{-1}$ of the water–methanol mixtures is linear ($r^2 > 0.99$). A linear trend for $pK_{aATN1}$ or $pK_{aPRO}$ could be achieved;

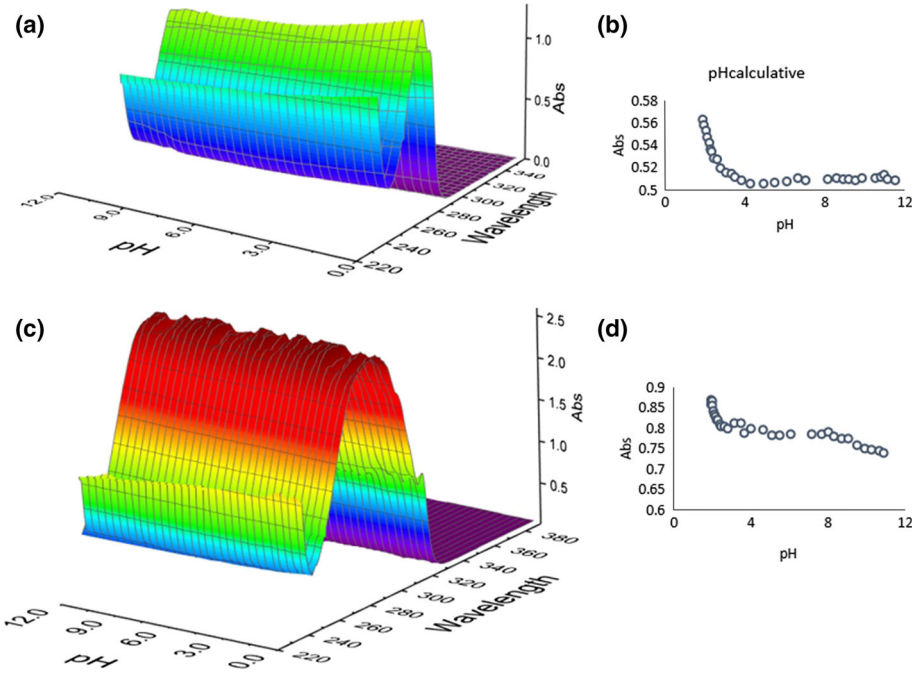


**Fig. 3** Experimental absorption spectra recorded in the course pH-metric titrations of (**a**) ATN and (**c**) PRO. Spectral data sets were acquired from their respective analytes in the concentration range $1.0 \times 10^{-3}$ mol·dm$^{-3}$–$3.0 \times 10^{-3}$ mol·dm$^{-3}$ in a 30% (v/v) MeOH–water binary solvent mixture, with the pH ranging from 1.8 to 12. In all cases temperature and ionic strength were held at 25 °C and 0.1 mol·dm$^{-3}$ of $NaClO_4$. (**b**) and (**d**) are average values of absorbance at different pH values in a range of wavelength 250–260 nm for ATN and PRO, respectively. Sampling was accomplished in flow-through quartz cells with 10 mm optical path length

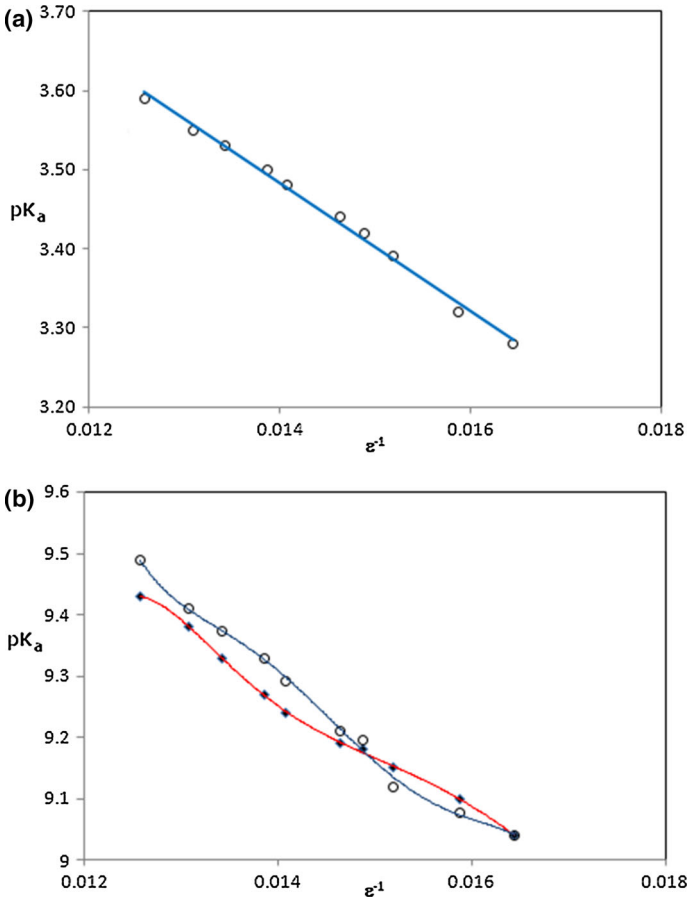


**Fig. 4** **a** Plot of $pK_{aATN2}$ versus $\varepsilon^{-1}$ of different mixed solvents performed in stable conditions of temperature and ionic strength. **b** Plots of $pK_{aATN1}$ (*red line*) and $pK_{aPRO}$ (*blue line*) versus $\varepsilon^{-1}$ of different mixed solvents performed in stable conditions of temperature and ionic strength [at 25 °C and an ionic strength of 0.1 mol·dm$^{-3}$ ($NaClO_4$)] (Color figure online)

however it yielded a far worse $r^2$ fit value. Therefore, we tested two more complex approaches (required to better understand solvent effects) that accounted for solvent–solvent and solute–solvent interactions. First, we tested two approaches to evaluate the solute–solvent interaction. In the first approach, the correlation between $pK_a$ and solvent polarity ($E_T$) was investigated. As seen from the plots of $pK_a$ versus $E_T$, Fig. 5, the relationship is nonlinear. We attributed this to the fact that water preferentially dissolves methanol compared to the solute [35, 36]. As the percentage of methanol was increased in the mixtures, the self-associated structure of water gradually breaks down and at the methanol-rich region, preferential solvation by water appears mainly because of solute–solvent hydrogen bonding. In the second approach we used a multi-parametric approach (KAT) developed by Kamlet et al. [37–39] to predict $pK_a$. The solvatochromic parameters used in this approach were the hydrogen-bond acidity ($\alpha$), hydrogen-bond basicity ($\beta$) and dipolarity/polarizability ($\pi^*$) of the water–methanol solvent mixtures. The latter term, $\pi^*$, is the index of the solvent polarizability, which is a measure of the ability of a solvent to

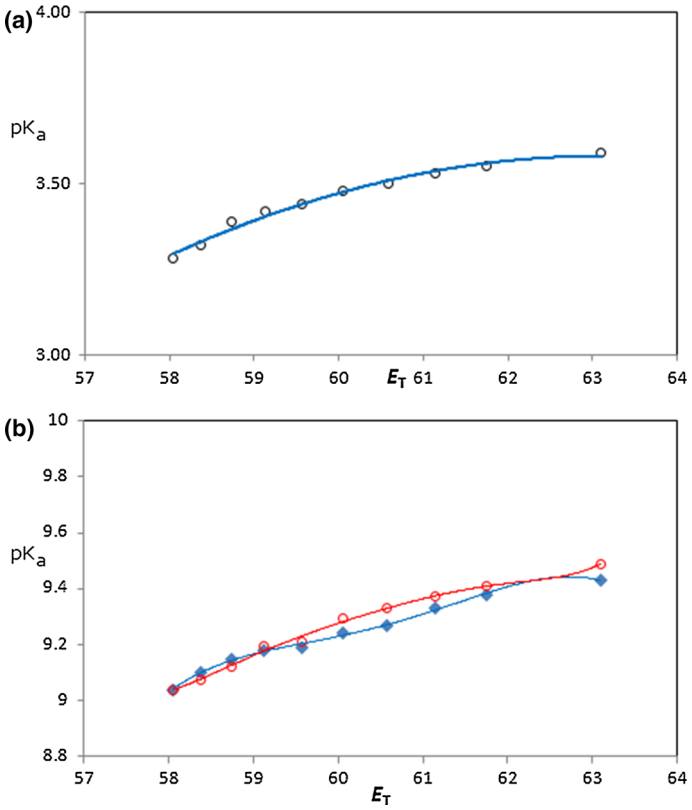


**Fig. 5** **a** Plot of $pK_{aATN2}$ versus the $E_T$ of different mixed solvents performed in stable conditions of temperature and ionic strength. **b** Plots of $pK_{aATN1}$ (*red line*) and $pK_{aPRO}$ (*blue line*) versus the $E_T$ of different mixed solvents at 25 °C and an ionic strength of 0.1 mol·dm$^{-3}$ ($NaClO_4$) (Color figure online)

stabilize a charge or a dipole by its own dielectric effects. The contributions of these parameters to the measured $pK_a$ values were determined from the plots of each property versus the mole fraction of the organic solvent (Table 2). Together, these parameters constitute more comprehensive measures of solvent character than $E_T$ or any other single physical parameter.

A general multi-parametric equation, Eq. 5, was used to predict $pK_a$ values

$$\log_{10}K = A_0 + a\alpha + b\beta + p\pi^* \tag{5}$$

where $A_0$ represents the regression value and $a$, $b$ and $p$ are the regression coefficients, which measure the relative susceptibilities of the solvent-dependence of $pK_a$ to $\alpha$, $\beta$, and $\pi^*$ parameters, respectively. The solvatochromic parameters ($\alpha$, $\pi^*$, and $\beta$) of Kamlet–Taft's scales vary from 0.0 to about 1 for these solvents.

Although $E_T$ is identified as the main contributor to variations of $pK_a$ values in binary water–organic solvents, the results show single-parameter correlations did not give good results based on their low $r^2$ values, 0.91–0.94, while the correlation analysis with dual-parameter equations shown in Eq. 6 indicates significant improvement:

**Table 2** Polarity and KAT solvatochromic parameters of different water–methanol mixtures [40, 41]

| Methanol % (v/v) | $E_T$ | ($\alpha$) hydrogen-bond acidity | ($\beta$) hydrogen-bond basicity | ($\pi^*$) dipolarity/ polarizability |
|---|---|---|---|---|
| 0 | 63.10 | 1.23 | 0.49 | 1.14 |
| 10 | 61.75 | 1.19 | 0.51 | 1.13 |
| 15 | 61.14 | 1.17 | 0.53 | 1.12 |
| 20 | 60.58 | 1.14 | 0.54 | 1.10 |
| 25 | 60.05 | 1.11 | 0.56 | 1.09 |
| 30 | 59.57 | 1.08 | 0.57 | 1.07 |
| 35 | 59.13 | 1.06 | 0.59 | 1.06 |
| 40 | 58.74 | 1.04 | 0.60 | 1.04 |
| 45 | 58.38 | 1.02 | 0.62 | 1.02 |
| 50 | 58.05 | 1.01 | 0.63 | 1.00 |

$$pK_{aPRO} = 6.99(\pm 0.24) + 0.92(\pm 0.35)\alpha + 1.14(\pm 0.56)\pi^* \quad (6a)$$

$$(N = 10,\ r^2 = 0.99,\ ose = 1.64 \times 10^{-2},\ rss = 1.87 \times 10^{-3},\ f\text{-test} = 253.8)$$

$$pK_{aATN2} = 1.23(\pm 0.82) - 0.03(\pm 0.50)\beta + 2.07(\pm 0.50)\pi^* \quad (6b)$$

$$(N = 10,\ r^2 = 0.99,\ ose = 1.09 \times 10^{-2},\ rss = 8.46 \times 10^{-4},\ f\text{-test} = 368.1)$$

$$pK_{aATN1} = 6.48\,(\pm 0.18) + 1.04\,(\pm 0.27)\,\alpha + 1.51(\pm 0.42)\,\pi^* \quad (6c)$$

$$(N = 10, r^2 = 0.99,\ ose = 1.25 \times 10^{-2},\ rss = 1.09 \times 10^{-3},\ f\text{-test} = 643.8)$$

where $N$, rss, ose and $r^2$ represent the number of the samples (mixed solvents), the residual sum of squares, the overall error and regression coefficient, respectively.

It can be seen from Table 1 that the dielectric constants of the solvent mixtures decrease as the solutions are enriched in organic solvent. The values of $pK_{aPRO}$ and $pK_{aATN2}$ and $pK_{aATN1}$ all decrease with decreasing dielectric constant of the medium. Nevertheless, this property is often inadequate to explain this variation as a single parameter. Therefore, a dual-parametric approach according to the KAT equation was applied to find out which parameter is responsible for this behavior. The positive $\pi^*$ coefficients in the correlation analysis of $pK_{aPRO}$, $pK_{aATN2}$ and $pK_{aATN2}$ by the KAT equation imply that a decrease in the polarity of the mixed solvents, decreases the protonation constant. This indicates the polarity parameter, $\pi^*$, is the most important (with a large difference of affinity with the donor or acceptor acidity or basicity parameters) in the correlation analysis of the $pK_a$ values of PRO and ATN. Furthermore, the positive coefficient of $\alpha$ or negative coefficient of $\beta$ in the correlation of $pK_a$ suggests that increasing basicity of the solvent mixtures decreases the $pK_a$ values of PRO and ATN as can be seen in Eq. 6.

In conjunction with the experimental determination of $pK_a$ values, quantum mechanical DFT calculations were also conducted. As discussed in the supporting information, solvation Gibbs energies ($G$) play an important role in prediction of molecular structures and $pK_a$ constants due to its relation to the tendency of the system to react or change. Since $\varepsilon$ is the most sensitive to change for different water–methanol solvent compositions, we

changed its value according to Table 1 for each binary solvent, in order to accurately evaluate $G$ for each drug molecule. The general form of the proton transfer reaction shown in the supporting information (Eq. S10) gives all possible $n$-hydrated species ($n = 0$–3) for PRO and ATN (Fig. 6). According to the results, the following reactions are the best match to those of experimental results.

$$\mathrm{ATN}: \mathrm{H_2L^{2+}} + \mathrm{OH^-(H_2O)_2} \rightleftharpoons \mathrm{HL^+(H_2O)_3} \tag{7}$$

$$\mathrm{ATN}: \mathrm{HL^+(H_2O)_2} + \mathrm{OH^-(H_2O)} \rightleftharpoons \mathrm{L(H_2O)_3} + \mathrm{H_2O} \tag{8}$$

$$\mathrm{PRO}: \mathrm{HL^+} + \mathrm{OH^-(H_2O)} \rightleftharpoons \mathrm{L(H_2O)} + \mathrm{H_2O} \tag{9}$$

In Eqs. 8 and 9, $\mathrm{L(H_2O)}_n$ and $\mathrm{HL^+(H_2O)}_n$ represent the neutral and the first protonated forms of ATN and PRO solvated with $n$ molecules of water, respectively, and in Eq. 7, $\mathrm{H_2L^{2+}}$ represents the second protonated form of ATN. Isolated $\mathrm{H_2O}$ molecules are shown as products in Eqs. 8 and 9.

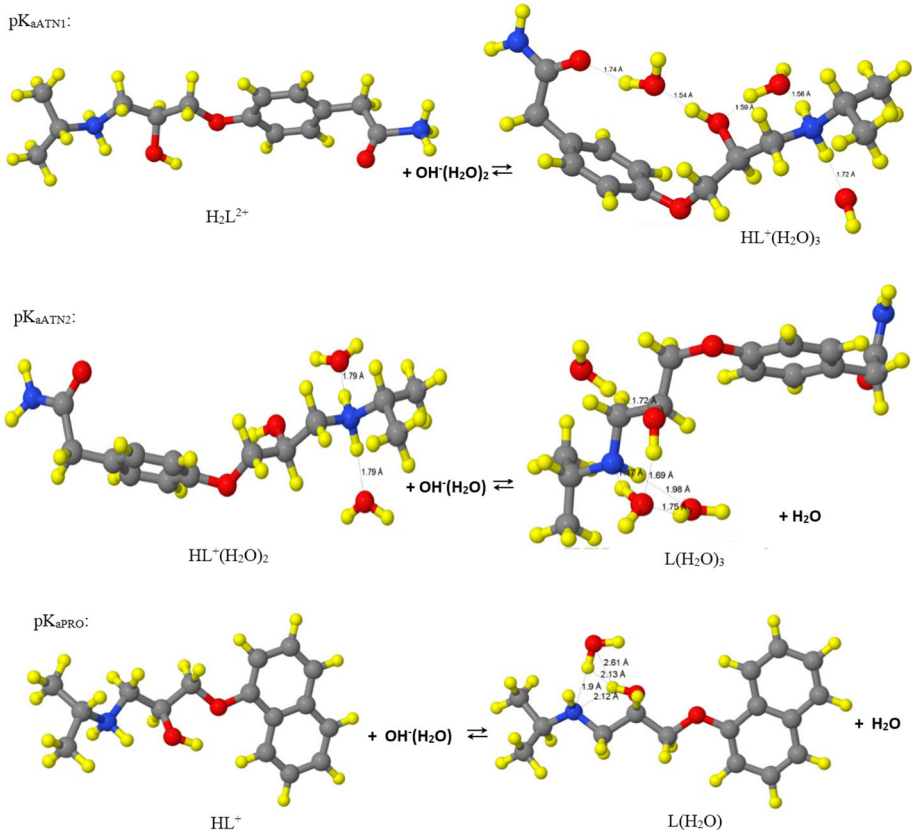


**Fig. 6** Selected optimized structures of bare and cluster ATN and PRO molecules at the DFT-B3LYP/6-311++G (d,p)/SMD level

$$\mathrm{RD} = \frac{\left|\mathrm{p}K_{\mathrm{cal}} - \mathrm{p}K_{\mathrm{exp}}\right|}{\mathrm{p}K_{\mathrm{exp}}} \tag{10}$$

$$\%\ \mathrm{MRD} = \sum \frac{\mathrm{RD}}{n} * 100 \tag{11}$$

The computational p$K_a$ values are listed in Table 1 and were compared with experimental p$K_a$ values by relative deviation (RD) and percentage of mean relative deviation (%MRD), which are defined in Eq. 10 and 11, respectively, with $n$ being the number of the samples (mixed solvents). The mean relative differences of 0.19, 0.09 and 0.41% between experiment and calculation for p$K_{aPRO}$, p$K_{aATN1}$ and p$K_{aATN2}$ strongly supported our model. Moreover, both methods capture the tendency of p$K_a$ to decrease with increasing percentage of methanol.

## 4 Conclusions

In this work p$K_a$ values of two important anti-hypertension drugs, ATN and PRO, were determined using a potentiometric method in various aqueous methanol mixtures. The solvent dependence of their acid–base equilibria were determined by UV-spectroscopy/potentiometric titration and correlations with the KAT solvatochromic parameters. Using linear relationships between these solvatochromic parameters and protonation constants, the p$K_a$ values were obtained with good accuracy. The experimental results are supplemented with DFT calculations, which provide a critical comparative evaluation of both the experimental determination of p$K_a$ and the computational prediction of p$K_a$ on ATN and PRO drugs. The cluster continuum method with implicit-explicit solvent molecules was used to calculate the p$K_a$ values in various binary mixtures of water and methanol, the total Gibbs energies were obtained for the ATN and PRO clusters at the DFT-B3LYP/6-311++G(d,p) level of theory. For applying the solvent effects on the species involved in the selected proton transfer reactions, the SMD solvation model was used. It is shown that there is a good correlation between experimental and theoretical results.

## References

1. Mozayani, A., Raymon, L.: Handbook of Drug Interactions: A Clinical and Forensic Guide, 1st edn. Springer, New Jersey (2004)
2. Narasimham, L., Barhate, V.D.: Physico-chemical characterization of some beta blockers and anti-diabetic drugs-potentiometric and spectrophotometric p$K_a$ determination in different co-solvents. Chem-Eur J. **2**, 36–46 (2011)
3. Uzel, S.G., Pavesi, A., Kamm, R.D.: Microfabrication and microfluidics for muscle tissue models. Prog. Biophys. Mol. Biol. **115**, 279–293 (2014)
4. Maitra, A., Bagchi, S.: Study of solute–solvent and solvent–solvent interactions in pure and mixed binary solvents. J. Mol. Liq. **137**, 131–137 (2008)
5. Soleimani, F., Karimi, R., Gharib, F.: Thermodynamic studies on protonation constant of acyclovir at different ionic strengths. J. Solution Chem. **45**, 920–931 (2016)
6. Atanassova, M., Billard, I.: Determination of p$K_a$ IL values of three chelating extractants in ILs: consequences for the extraction of 4f elements. J. Solution Chem. **44**, 606–620 (2015)
7. Dávila, Y.A., Sancho, M.I., Almandoz, M.C., Blanco, S.E.: Solvent effects on the dissociation constants of hydroxyflavones in organic–water mixtures. Determination of the thermodynamic p$K_a$ values by UV–visible spectroscopy and DFT calculations. J. Chem. Eng. Data **58**, 1706–1716 (2013)

8. Signore, G., Nifosì, R., Albertazzi, L., Storti, B., Bizzarri, R.: Polarity-sensitive coumarins tailored to live cell imaging. J. Am. Chem. Soc. **132**, 1276–1288 (2010)
9. Kudo, K., Momotake, A., Tanaka, J.K., Miwa, Y., Arai, T.: Environmental polarity estimation in living cells by use of quinoxaline-based full-colored solvatochromic fluorophore PQX and its derivatives. Photech. Photobio. Sci. **11**, 674–678 (2012)
10. Giusti, L.A., Marini, V.G., Machado, V.G.: Solvatochromic behavior of 1-(*p*-dimethylaminophenyl)-2-nitroethylene in 24 binary solvent mixtures composed of amides and hydroxylic solvents. J. Mol. Liq. **150**, 9–15 (2009)
11. Farajtabar, A., Jaberi, F., Gharib, F.: Preferential solvation and solvation shell composition of free base and protonated 5,10,15,20-tetrakis(4-sulfonatophenyl) porphyrin in aqueous organic mixed solvents. Spectrochim. Acta A **83**, 213–220 (2011)
12. Takamuku, T., Saisho, K., Nozawa, S., Yamaguchi, T.: X-ray diffraction studies on methanol–water, ethanol–water, and 2-propanol–water mixtures at low temperatures. J. Mol. Liq. **119**, 133–146 (2005)
13. Jaberi, F., Gharib, F.: Spectrophotometric determination of equilibrium constants of dimethyl and diethyltin(IV) dichloride with 5,10,15,20-tetrakis(4-trimethyl-ammonio-phenyl)-prophine eetratosylate. J. Solution Chem. **44**, 34–44 (2015)
14. Naderi, F., Farajtabar, A., Gharib, F.: Solvatochromic and preferential solvation of fluorescein in some water–alcoholic mixed solvents. J. Mol. Liq. **190**, 126–132 (2014)
15. Gharib, F., Abbaszadeh, M., Pousti, M.: Acid–base properties of adenosine 5′-monophosphate, guanosine 5′-monophosphate, and inosine 5′-monophosphate in aqueous solutions of methanol. Helv. Chim. Acta **96**, 1134–1145 (2013)
16. Naderi, F., Farajtabar, A., Gharib, F.: Protonation of tetrakis(4-sulfonatophenyl) porphyrin in aqueous solutions of scetonitrile and dioxane. J. Solution Chem. **41**, 1033–1043 (2012)
17. Jabbari, M., Gharib, F.: Solvent dependence on antioxidant activity of some water-insoluble flavonoids and their cerium(IV) complexes. J. Mol. Liq. **168**, 36–41 (2012)
18. Avdeef, A.: Absorption and drug development: solubility, permeability, and charge state. Wiley, New York (2012)
19. Beale, J.M., Block, J., Hill, R.: Organic Medicinal and Pharmaceutical Chemistry, 12th edn. Lippincott Williams and Wilkins, Philadelphia (2010)
20. Leggett, D.J.: Computation Methods for the Determination of Formation Constants. Plenum Press, New York (1985)
21. Meloun, M., Javůrek, M., Havel, J.: Multiparametric curve fitting—X: a structural classification of programs for analysing multicomponent spectra and their use in equilibrium-model determination. Talanta **33**, 513–524 (1986)
22. Gordon, M.S., Schmidt, M.W.: Advances in electronic structure theory Gamess a decade later. In: Dykstra, C.E., Frenking, G., Kim, K.S., G.E. Scuseria, G.E. (eds.) Theory and Applications of Computational Chemistry, pp. 1185–1189. Elsevier, Amsterdam (2005)
23. Pliego, J.R., Riveros, J.M.: Theoretical calculation of p$K_a$ using the cluster-continuum model. J. Phys. Chem. A **106**, 7434–7439 (2002)
24. Jacquemin, D., Perpète, E.A.: Ab initio calculations of the colour of closed-ring diarylethenes: TD-DFT estimates for molecular switches. Chem. Phys. Lett. **429**, 147–152 (2006)
25. Allouche, A.R.: Gabedit—A graphical user interface for computational chemistry softwares. J. Comput. Chem. **32**, 174–182 (2011)
26. Hanson, R.M., Prilusky, J., Renjian, Z., Nakane, T., Sussman, J.L.: JSmol and the next-generation web-based representation of 3D molecular structure as applied to Proteopedia. Isr. J. Chem. **53**, 207–216 (2013)
27. Bode, B.M., Gordon, M.S.: MacMolPlt: a graphical user interface for GAMESS. J. Mol. Graph. Model. **16**, 133–138 (1998)
28. Kiani, F., Rostami, A.A., Sharifi, S., Bahadori, A., Chaichi, M.J.: Determination of acidic dissociation constants of glycine, valine, phenylalanine, glycylvaline, and glycylphenylalanine in water using ab initio methods. J. Chem. Eng. Data **55**, 2732–2740 (2010)
29. Maleki, N., Haghighi, B., Safavi, A.: Evaluation of formation constants, molar absorptivities of metal complexes, and protonation constants of acids by nonlinear curve fitting using microsoft excel solver and user-defined function. Microchem. J. **62**, 229–236 (1999)
30. Babić, S., Horvat, A.J., Pavlović, D.M., Kaštelan-Macan, M.: Determination of p$K_a$ values of active pharmaceutical ingredients. Trac-Trend Anal. Chem. **26**, 1043–1061 (2007)
31. Schurmann, W., Turner, P.: Membrane model of the human oral mucosa as derived from buccal absorption performance and physicochemical properties of the beta-blocking drugs atenolol and propranolol. J. Pharm. Pharmacol. **30**, 137–147 (1978)

32. Völgyi, G., Ruiz, R., Box, K., Comer, J., Bosch, E., Takács-Novák, K.: Potentiometric and spectrophotometric p$K_a$ determination of water-insoluble compounds: validation study in a new cosolvent system. Anal. Chim. Acta **583**, 418–428 (2007)
33. Sanli, S., Altun, Y., Guven, G.: Solvent effects on p$K_a$ values of some anticancer agents in acetonitrile–water binary mixtures. J. Chem. Eng. Data **59**, 4015–4020 (2014)
34. Farajtabar, A., Gharib, F.: Spectral analysis of naringenin deprotonation in aqueous ethanol solutions. Chem. Pap. **67**, 538–545 (2013)
35. Reichardt, C.: Solvents and Solvent Effects in Organic Chemistry, 3rd edn. Wiley-VCH, Weinheim (2004)
36. Marcus, Y.: Water structure enhancement in water-rich binary solvent mixtures. Part II. The excess partial molar heat capacity of the water. J. Mol. Liq. **166**, 62–66 (2012)
37. Kamlet, M.J., Gal, J.F., Maria, P.C., Taft, R.W.: Linear solvation energy relationships. Part 32. A coordinate covalency parameter, ξ, which, in combination with the hydrogen bond acceptor basicity parameter, $\beta$, permits correlation of many properties of neutral oxygen and nitrogen bases (including aqueous p$K_a$). J. Chem. Soc. Perkin Trans. **2**, 1583–1589 (1985)
38. Kamlet, M.J., Carr, P.W., Taft, R.W., Abraham, M.H.: Linear solvation energy relationships. 13. Relationship between the Hildebrand solubility parameter, $\Delta H$, and the solvatochromic parameter, π*. J. Am. Chem. Soc. **103**, 6062–6066 (1981)
39. Kamlet, M.J., Abboud, J.L.M., Abraham, M.H., Taft, R.W.: Linear solvation energy relationships. 23. A comprehensive collection of the solvatochromic parameters, π*, α, and β, and some methods for simplifying the generalized solvatochromic equation. J. Org. Chem. **48**, 2877–2887 (1983)
40. Taft, R.W., Abboud, J.L.M., Kamlet, M.J.: Linear solvation energy relationships. An analysis of Swain's solvent" acity" and" basity" scales. J. Org. Chem. **49**, 2001–2005 (1984)
41. Deb, N., Shannigrahi, M., Bagchi, S.: Use of fluorescence probes for studying Kamlet-Taft solvatochromic parameters of micellar system formed by binary mixture of sodium dodecyl sulfate and Triton-X 100. J. Phys. Chem. B **112**, 2868–2873 (2008)